Original Research

Gene expression profiling in glomeruli of diabetic nephropathy rat

Qian Zhang, Xinhua Xiao, Ming Li, Wenhui Li, Miao Yu, Huabing Zhang, Xiaofang Sun, Lili Mao and Hongding Xiang

Key Laboratory of Endocrinology, Ministry of Health, Department of Endocrinology, Peking Union Medical College Hospital, Peking Union Medical College, Chinese Academy of Medical Sciences, No. 1 Shuaifu Garden, Beijing 100730, China
Corresponding author: Xinhua Xiao. Emails: xiaoxinhua@medmail.com.cn or xiaoxinhua@hotmail.com

Abstract

Diabetic nephropathy (DN) remains the most common cause of end-stage renal disease (ESRD) as the burden of diabetes increases worldwide. To find improved intervention strategies for this disease, it is necessary to investigate the molecular mechanisms involved. To obtain more insight into processes that lead to DN, mRNA expression profiles of diabetic and normal glomeruli from rat kidneys were compared. Rats were divided into a control group and a DN group randomly. The DN group was injected with streptozotocin. Fasting blood glucose (FBG) and weight were measured monthly. On the 12th week, blood samples were collected and analyzed for plasma creatinine and blood urea nitrogen (BUN). Glomeruli were isolated and Illumina Rat Ref-12 V1.0 Expression Beadchip gene array was performed. Quantitative realtime polymerase chain reaction (Q-RT-PCR) was used to confirm the results of gene array for a selected number of genes. We found FBG, 24-h urinary albumin, serum creatinine and BUN were significantly increased, while urinary creatinine and body weight were significantly decreased in the DN group. Glomeruli from the DN group had 624 genes with differential expression. DAVID (Database for Annotation, Visualization and integrated Discovery) analysis showed that the three most enriched terms were 'cytosol' (GO:0005829), 'translational elongation' (GO:0006414) and 'mitochondion' (GO:0005739). Those genes could be mapped to eight pathways. The most common type of enriched pathway was related to 'extracellular matrix (ECM)-receptor interaction'. Other pathways included those for 'ribosome', 'focal adhesion', 'oxidative phosphorylation', 'transforming growth factor (TGF)-beta signaling pathway', 'Parkinson's disease', 'Alzheimer's disease' and 'renin–angiotensin system'. Q-RT-PCR verified that *Atp5b* (F1-ATPase beta subunit), *Col1a1* (collagen type 1 alpha 1), *Cox6c* (cytochrome c oxidase subunit VIc), *Ndufs3* (NADH dehydrogenase [ubiquinone] Fe-S protein 3) and *Tgfb1* (transforming growth factor β1) were significantly up-regulated in the DN group. The expressions of NDUFS3 and TGF-β1 in DN rats were increased. Our findings suggested that the oxidative phosphorylation pathway, ECM-receptor interaction, TGF-β pathway and renin–angiotensin system may be involved in the development of DN.

Keywords: hyperglycemia, diabetic nephropathy, gene array, oxidative phosphorylation

Experimental Biology and Medicine 2012; **237**: 903–911. DOI: 10.1258/ebm.2012.012032

Introduction

Diabetes mellitus (DM) is considered to be a metabolic disorder with different etiologies characterized by hyperglycemia resulting from defects in insulin secretion and/or action. In 2000, 171 million cases of DM worldwide were estimated, and that number is expected to increase to 366 million cases in 2030.[1] The increasing prevalence of DM has led to a growing number of chronic complications, including diabetic nephropathy (DN).[2] Approximately 30% of patients with either type 1 or type 2 DM develop DN.[3] DN is the single most common cause of end-stage renal disease (ESRD) in adults.[4] The lifetime risk of developing DN with progression to ESRD is roughly equivalent in type 1 and type 2 DM.[5] The presence of DN heralds a marked increase in patient morbidity and premature mortality, and significantly impacts cost of care.[6] While mortality with diabetic renal disease can precede progression to ESRD, diabetes in those with ESRD remains a significant predictor for increased cardiovascular risk and mortality.[4]

DN is characterized by a set of diabetic pathophysiological changes, which begin with glomerular hyperfiltration and renal hypertrophy, and then progress to proteinuria and glomerular filtration rate reduction. As the molecular mechanisms leading to ESRD in DN are still unknown, treatment of DN becomes complex and the therapeutic goal is difficult to achieve.

Gene expression profiling using microarray analysis has been used to study biological signaling pathways in many

studies. Although gene-profiling studies have been described in streptozotocin (STZ)-induced diabetic CD-1 mouse models[7] and non-obese diabetic mouse models[8] using whole kidneys, these studies provide initial insights into early global changes in the diabetic kidney. Little is known about the molecular and temporal events occurring specifically in glomeruli. Glomerular sclerosis and fibrosis caused DN through the metabolic and hemodynamic changes of DM. Microarray studies of glomeruli in STZ-induced diabetic rats have not been reported.

In the present study, we used the Illumina Rat Ref-12 V1.0 Expression Beadchip gene array on glomeruli of STZ-induced diabetic rats to study the genes with differential expressions and their function categories for diabetic and normal rats in glomeruli. Our present study provides further information on the pathogenesis of DN and offers specific molecular targets for DN diagnosis, prevention, clinical treatment and drug design.

Materials and methods

Experimental DN rats

Twenty male Sprague-Dawley rats, weighing 200–250 g (from the Institute of Laboratory Animal Sciences, Chinese Academy of Medical Sciences & Peking Union Medical College, Beijing, China; SCXK-2011-0010) were randomly divided into two groups: a DN group and a control group ($n = 10$ in each group). Following the study of Onozato *et al.*,[9] the DN group was administered a single dose of STZ, 60 mg/kg, via the tail vein, formulated in 0.1 mmol/L citrate buffer, pH 4.5 (Sigma-Aldrich, St Louis, MO, USA). A week after the injection, the six-hour fasting blood glucose (FBG) concentration of the DN rats was measured to confirm hyperglycemia. All animals were housed in an environmentally controlled room at 25°C in a 12-h light/dark cycle and given free access to food and water throughout the experimental period. The body weight, blood glucose and 24-h urine tests were measured every four weeks. Fasting animals were allowed free access to water. Twelve weeks after the injection of STZ, blood samples were taken from the rats under anesthesia. The rats were then sacrificed and their left kidneys were weighed. An index of renal hypertrophy was estimated by comparing the weight of the left kidney to the body weight. Then some kidney tissues were collected. Glomeruli were isolated by using a conventional sieving method.[10] In brief, kidneys were minced well on ice and forced through sequential steel sieves, and glomeruli were collected with the use of cold phosphate-buffered saline (PBS), transferred to a tube and pelleted for one minute at 1200 *g*. The supernatant was removed, and then glomeruli were stored in dry ice to perform the microarray and quantitative realtime polymerase chain reaction (Q-RT-PCR) experiment. Some kidneys were fixed in 10% neutralized formalin for histology. All procedures involving animals were approved by the Animal Care and Use Committee of the Peking Union Medical College Hospital (Beijing, China, MC-07-6004) and were conducted in compliance with Guide of the Care and Use of Laboratory Animals (NIH publication No. 23–86, revised 1996). All surgery was performed under sodium pentobarbital anesthesia, and all efforts were made to minimize suffering.

Body weight and FBG concentrations

The body weight was monitored every four weeks. The six-hour FBG concentration was measured every four weeks by using a BREEZE 2 glucometer (Bayer, Leverkusen, Germany) with blood from a tail bleed.

Urine tests

The 24-h urine samples were collected at the 12th week. The rats were housed in metabolic cages for 24 h to collect urine samples. Urine samples were centrifuged at 3000 *g* for 10 min (Heraeus Varifuge 3.0; Hamburg, Germany) to remove any suspended particles and stored in aliquots at −80°C. Urine protein and creatinine levels were measured with an Olympus AU 5400 analyzer (Olympus Diagostica, Hamburg, Germany).

Serum biochemistry analysis

At the 12th week, after euthanasia, blood samples were taken. The blood samples were centrifuged at 3000 *g* for 10 min (Heraeus Varifuge 3.0), and serum was stored in aliquots at −80°C. Serum creatinine and blood urea nitrogen (BUN) were measured with an Olympus AU 5400 analyzer.

Renal histological analysis

The kidneys from the control and DN groups ($n = 10$ in each group) were removed and embedded in paraffin to prepare 4 μm tissue slices. The tissue slices were stained with periodic acid-Schiff for histological evaluation. The mesangial expansion index was scored in four levels from 0 to 3, with the index scores defined as follows:[11] 0, normal glomeruli; 1, matrix expansion occurred in up to 50% of a glomerulus; 2, matrix expansion occurred in 50–75% of a glomerulus; 3, matrix expansion occurred in 75–100% of a glomerulus from kidney slices of each rat, and then the means were calculated.

RNA preparation and microarray experiments

Glomeruli were taken from the DN and control groups ($n = 3$ in each group) to perform the microarray experiments. Before the microarray experiment, each total RNA was processed with RNase-free DNase (Qiagen, Valencia, CA, USA). RNA was reverse-transcribed by superscript II (Invitrogen, Carlsbad, CA, USA). The Illumina RatRef-12 Expression BeadChip contains 22,524 probes for a total of 22,228 rat genes selected primarily from the NCBI RefSeq database (Release 16; Illumina, San Diego, CA, USA), and was used in accordance with the manufacturer's instructions. All reagents were optimized for use with Illumina's Whole-Genome Expression platform. Total RNA of 200 ng was used for cRNA *in vitro* transcription and labeling with

Table 1 Oligonucleotide sequences for quantitative realtime polymerase chain reaction analysis

Gene symbols	Forward primer	Reverse primer
Atp5b	ACCACCAAGAAGGGCTCGAT	GCATCCAAATGGGCAAAGG
Col1a1	TGGCAAGAACGGAGATGA	AGCTGTTCCAGGCAATCC
Cox6c	CAGCTTTGTATAAGTTTCGTGTGG	ACCAGCCTTCCTCATCTCCT
Ndufs3	GGCTTCGAGGGACATCCTTT	CCFCTTCACCTCATCGTCAT
Tgfb1	ATACGCCTGAGTGGCTGTCT	TGGGACTGATCCCATTGATT
Gadph	GACCCCTTCATTGACCTCAAC	CGCTCCTGGAAGATGGTGATG

Atp5b, F1-ATPase beta subunit; *Col1a1*, collagen type 1 alpha 1; *Cox6c*, cytochrome c oxidase subunit VIc; *Ndufs3*, NADH dehydrogenase (ubiquinone) Fe-S protein 3; *Tgfb1*, transforming growth factor beta 1; *Gadph*, glyceraldehyde-3-phosphate dehydrogenase

the TotalPrep™ RNA Labeling Kit using Biotinylated-UTP (Ambion, Austin, TX, USA). Hybridization was carried out in Illumina Intellihyb chambers at 58°C for 18.5 h, followed by washing and staining, in accordance with the Illumina Hybridization System Manual. The signal was developed by staining with Cy3-streptavidin. The BeadChip was scanned on a high resolution Illumina BeadArray reader, using a two-channel, 0.8 μm resolution confocal laser scanner.

Data extraction and normalization

Illumina BeadStudio software (Version 2.0) was used to extract and normalize the expression data (fluorescence intensities) for the mean intensity of all arrays. Genes expressed in all arrays were selected for analyses. Normalized data were analyzed using the *t*-test and logistic regression.

Gene array data analysis

Subsequently, signals were averaged for glomeruli from the DN and control rats. DiffScore and Illumina Custom from the BeadStudio software package were used to determine the differentially expressed genes. The DiffScore was defined using the following formula: $10 \times \text{sgn}(\mu\text{cond} - \mu\text{ref}) \times [\log 10(p)]$. We established the following two criteria, based on the instructions of the Illumina platform, to identify the differentially expressed genes: (1) detection P value <0.01 in either of the two sample groups; (2) DiffScore >13 (corresponding to P value <0.05), under the Benjamini & Hochberg false discovery rate (FDR) correction for multiple tests.[12] Cluster analysis (Stanford University, Palo Alto, CA, USA) was done using software developed by Eisen *et al*.[13] To assign biological meaning to the group of genes with changed expression, the subset of genes which met the above criteria was analyzed with the gene ontology (GO) classification system, using Database for Annotation, Visualization, and integrated Discovery (DAVID) software (http://david.abcc.ncifcrf.gov/),[14] as well as Kyoto Encyclopedia of Genes and Genomes (KEGG). All thresholds in our analyses were set to 0.001. Over-representation of genes with altered expression within specific GO categories was determined using the one-tailed Fisher exact probability modified by the addition of a jack-knifing procedure, which penalizes the significance of categories with very few (e.g. one or two) genes and favors more robust categories with larger numbers of genes.[15]

Q-RT-PCR analysis

For validation of the microarray results, five genes from the gene list were selected for Q-RT-PCR analyses. Each Q-RT-PCR assay was repeated using three biological replicates and each analysis consisted of three technical replicates. Before PCR, each total RNA was processed with RNase-free DNase (Qiagen, Valencia, CA, USA). RNA was reverse-transcribed by Superscript II (Invitrogen). The primers were designed using Applied Biosystems (Foster City, CA, USA) Primer Express™ design software. Primers were purchased from Applied Biosystems. The reaction production could be accurately measured in the exponential phase of amplification by the ABI prism 7700 Sequence Detection System, with the following cycling conditions: an initial denaturation at 48°C for 30 min, 95°C for 15 min, 40 cycles of 95°C for 15 s, 55°C for one minute and a final unlimited 4°C hold. The sequences of the primers used are listed in Table 1. The signal of the housekeeping gene glyceraldehyde-3-phosphate dehydrogenase was used for normalization. Relative quantification of the mRNA between DN and control rats was calculated by the comparative Ct method.[16]

Immunohistochemistry staining

Renal tissues from the control and DN groups ($n = 10$ in each group) were fixed in 10% neutral buffered formalin, cast in paraffin, sliced into 4 μm sections and placed onto microscope slides. After removal of the paraffin by xylene and dehydration by graded alcohol, slides were immersed into distilled water. Kidney sections were then transferred into a 10 mmol/L citrate buffer solution (pH 6.0) and heated at 80°C for five minutes for antigen retrieval. After washing, 3.0% peroxide was applied for 20 min to block the activity of endogenous peroxidase. To avoid non-specific staining, the sections were incubated in blocking solution (5% bovine serum albumin) for one hour at room temperature, followed by treatment with rabbit polyclonal anti-NADH dehydrogenase (ubiquinone) Fe-S protein 3 (NDUFS3) antibody (1:50, 15066–1-AP; Proteintech Group, Chicago, IL, USA) or rabbit polyclonal antitransforming growth factor beta 1 (TGF-β1) antibody (1:50, 18978–1-AP; Proteintech Group), where indicated overnight at 4°C. Negative control sections were stained under identical conditions by substituting the primary antibody with equivalent concentrations of normal rabbit IgG. After washing with PBS, the slides were incubated with the labeled streptavidin biotin reagent, following the manufacturer's instructions.

Table 2 Body weight (g) of rats during three months

Groups	Zero month	One month	Two months	Three months
Control	223.5 ± 16.3	252.1 ± 16.0	248.3 ± 14.1	293.8 ± 17.9
DN	239.2 ± 15.7	257.3 ± 14.6*	246.1 ± 14.6**	264.5 ± 11.6**

Data represent mean ± SD ($n = 10$). *$P < 0.05$ versus the control group, **$P < 0.01$ versus the control group

Table 3 Fasting blood glucose (mmol/L) of rats during three months

Groups	One week	One month	Two months	Three months
Control	6.7 ± 0.5	6.2 ± 0.3	6.4 ± 0.3	6.4 ± 0.2
DN	19.7 ± 3.6**	18.3 ± 4.0**	19.9 ± 5.4**	20.4 ± 6.3**

Data represent mean ± SD ($n = 10$). **$P < 0.01$ versus the control group

Immunoreactive products were made visible by diaminobenzidine reaction. Sections were counterstained with hematoxylin for 15 s. Brownish-yellow granular or linear deposits were interpreted as positive areas. To evaluate the immunostaining, a total of more than 30 randomly chosen glomeruli per rat was coded and graded in a blind manner. Each score reflects changes in the extent rather than the intensity of staining and depends on the percentage of positive glomeruli. The degrees of NDUFS3 and TGF-β1 expression in 10 rats from each group were graded as follows: 0, absent or less than 25% staining; 1, 25–50% positive staining; 2, 50–75% positive staining; 3, more than 75% positive staining.[17]

Statistical analysis

All results are expressed as mean ± standard deviation (SD). Statistical analysis was performed with analysis of variance followed by a Student's *t*-test. $P < 0.05$ was considered statistically significant. Analysis was done with SPSS 11.0 (SPSS, Inc., Chicago, IL, USA).

Results

Body weight loss and fasting hyperglycemia in DN rats

On the day of injection of STZ, no significant differences were noted between the initial body weight of the DN group and the control group. However, the mean body weight of DN rats decreased significantly compared with the control rats at one month ($P < 0.05$), two months ($P < 0.01$) and three months ($P < 0.01$) after injection of STZ (Table 2). The FBG concentrations of the DN group were significantly higher than those of the control group at one month ($P < 0.01$), two months ($P < 0.01$) and three months ($P < 0.01$) after injection of STZ (Table 3).

Kidney dysfunction in DN rats

Three months after injection of STZ, urinary creatinine of the DN group was significantly suppressed ($P < 0.05$), whereas 24-h urinary albumin, serum creatinine and BUN in the DN group became significantly elevated compared with the control group ($P < 0.05$, Figure 1).

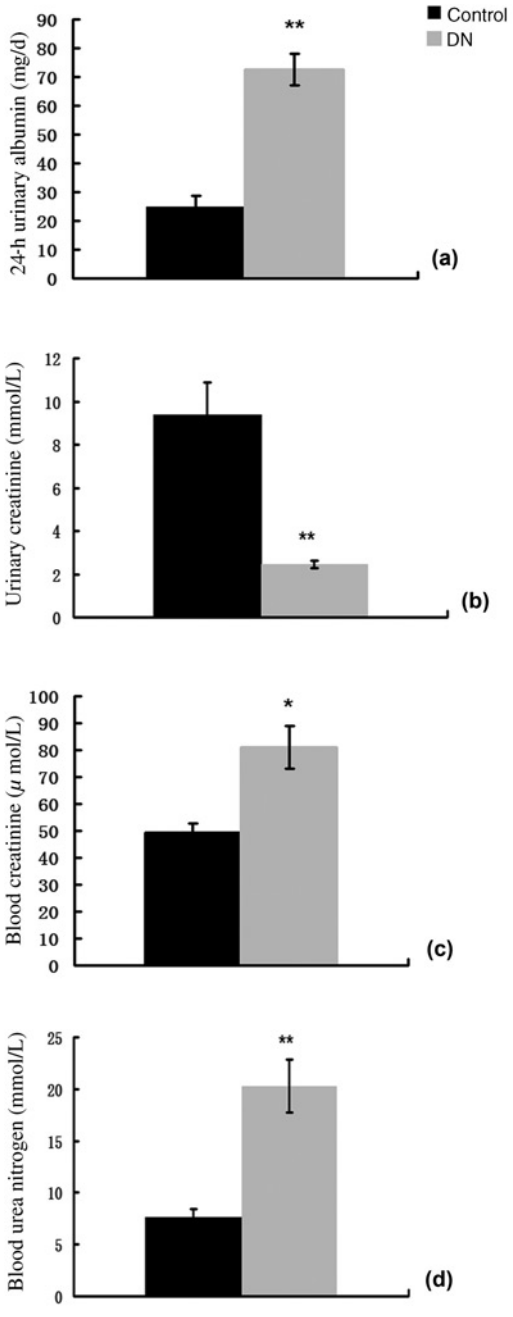

Figure 1 At the 12th week, 24-h urinary albumin (a), urinary creatinine (b), serum creatinine (c) and serum urea nitrogen (d) in rats. Urinary creatinine of the diabetic nephropathy (DN) group ($n = 10$ in each group) was significantly suppressed, whereas 24-h urinary albumin, serum creatinine and serum urea nitrogen of the DN group became significantly elevated compared with the control group ($n = 10$ in each group). Data represent mean ± SD ($n = 10$). *$P < 0.05$, **$P < 0.01$ versus the control group

Table 4 Hypertrophy-related parameters in DN rats

Groups	Left kidney weight (g)	Left kidney weight/body weight (mg/g)
Control	1.7 ± 0.1	3.2 ± 0.3
DN	3.6 ± 0.2*	8.2 ± 0.4*

DN, diabetic nephropathy
Data represent mean ± SD ($n = 10$). *$P < 0.05$ versus the control group

Kidney hypertrophy in DN rats

At the end of the study period, the mean left kidney weight and the ratio of left kidney weight to body weight of DN rats were significantly increased compared with the control group ($P < 0.05$, Table 4).

Renal histology in DN rats

The control group had normal histology (Figure 2a), while histological examination of the diabetic rats' kidneys revealed marked histological changes in the glomerular and tubular structures (Figure 2b and c).

Genes differentially expressed between DN and control groups

In this study, gene expression profiles in glomeruli from the rats were determined using whole genome-wide gene expression microarray analyses. Both the diabetic and control group contained three biological replicates, and therefore, a total of six microarrays were analyzed.

As a result, 624 differentially expressed genes were identified in glomeruli (Supplementary Table 1; please see http://ebm.rsmjournals.com/lookup/suppl/doi:10.1258/ebm.2012.012032/-/DC1). Clustering based on similarity in gene expression using all differentially expressed genes highlighted the difference in the transcriptional profiles between the DN and control groups.

To evaluate the pathophysiological associations of gene expression profiles, the most significantly enriched biological functions among differentially expressed genes were identified. DAVID analysis of all changed genes yielded 21 GO categories (cut-off FDR < 0.001, Table 5). The most enriched three term was 'cytosol' (GO:0005829), 'translational elongation' (GO:0006414) and 'mitochondion' (GO:0005739). There were 88 (FDR = 4.25E-11), 23 (FDR = 5.22E-11) and 93 (FDR = 1.82E-10) genes from glomeruli associated with these terms, respectively.

The aforementioned DAVID annotation tool was used for identification of putative KEGG pathways. The genes could be mapped to eight pathways (FDR < 0.001, Table 6). The most common type of enriched pathways was related to 'extracellular matrix (ECM)–receptor interaction' (FDR = 3.89E-13). The second most abundant category was related to 'ribosome' (FDR = 7.49E-09). Other pathways included those for 'focal adhesion' (FDR = 3.67E-06), 'oxidative

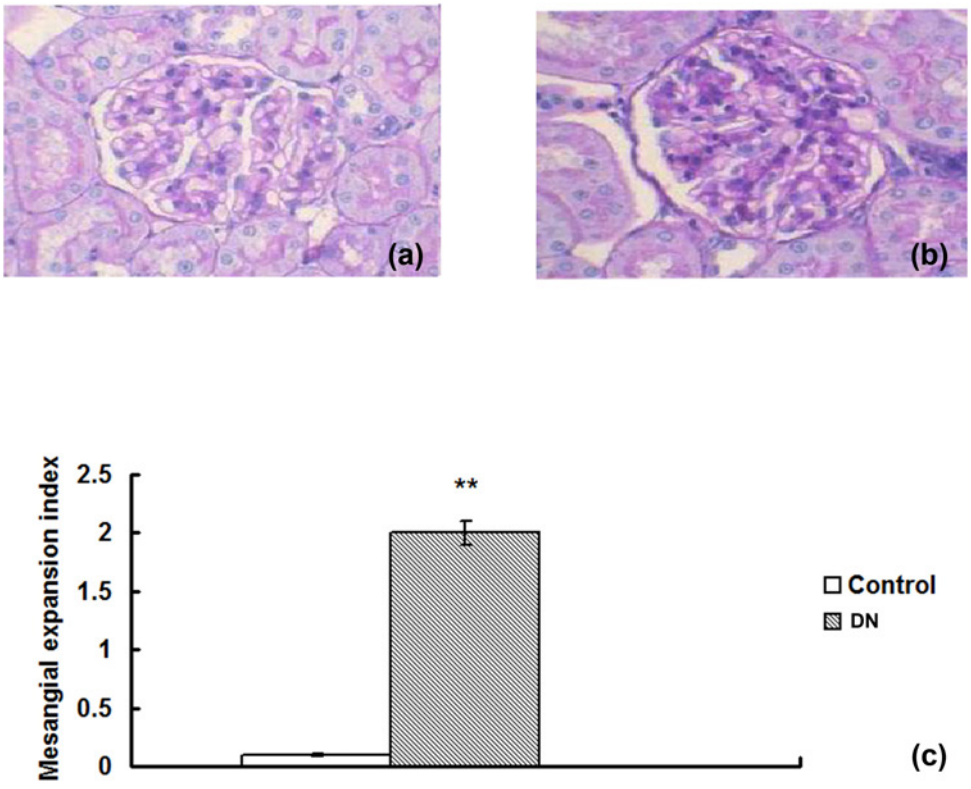

Figure 2 Histological staining with peridic acid-Schiff in glomeruli (a–c, original magnification, 200×) shows the glomerular and tubuloiterstitial structure of the control group (a) and diabetic nephropathy group (b). Expansion of the glomerular matrix was scored using four levels and an average value was obtained from analyses of more than 30 glomeruli per rat (c). The images were taken at the same size. Data represent mean ± SD ($n = 10$). **$P < 0.01$ versus the control group. (A color version of this figure is available in the online journal)

Table 5 Gene ontology groups with significant over-representation among genes with significantly changed expression in diabetic nephropathy (fold enrichment > 2, FDR < 0.001)

GO classification	GO term	GO ID	Count	Fold enrichment	FDR
Biological process	Translational elongation	GO:0006414	23	8.223	5.22E-11
	Translation	GO:0006412	40	3.174	4.84E-07
	Generation of precursor metabolites and energy	GO:0006091	25	3.567	2.36E-04
Cellular Constituent	Cytosol	GO:0005829	88	2.323	4.25E-11
	Mitochondrion	GO:0005739	93	2.196	1.82E-10
	Mitochondrial part	GO:0044429	54	3.095	2.98E-10
	Mitochondrial inner membrane	GO:0005743	35	3.651	1.37E-07
	Mitochondrial envelope	GO:0005740	41	3.127	3.03E-07
	Mitochondrial membrane	GO:0031966	39	3.180	5.72E-07
	Organelle inner membrane	GO:0019866	35	3.432	7.30E-07
	Ribosome	GO:0005840	36	3.201	2.60E-06
	Envelope	GO:0031975	47	2.518	1.40E-05
	Organelle envelope	GO:0031967	46	2.482	3.19E-05
	Organelle membrane	GO:0031090	65	2.039	5.00E-05
	Ribonucleoprotein complex	GO:0030529	41	2.382	6.60E-04
	Ribosomal subunit	GO:0033279	15	5.335	8.63E-04
Molecular function	Monovalent inorganic cation transmembrane transporter activity	GO:0015077	18	6.587	2.04E-06
	Hydrogen ion transmembrane transporter activity	GO:0015078	17	6.559	7.05E-06
	Structural constituent of ribosome	GO:0003735	30	3.573	7.62E-06
	Inorganic cation transmembrane transporter activity	GO:0022890	20	5.035	2.07E-05
	Structural molecule activity	GO:000519	42	2.579	5.80E-05

FDR, false discovery rate; GO, gene ontology

phosphorylation' (FDR = 4.91E-06), 'TGF-beta signaling pathway' (FDR = 7.11E-06), 'Parkinson's disease' (FDR = 2.35E-04), 'Alzheimer's disease' (FDR = 3.28E-04) and 'renin–angiotensin system (RAS)' (FDR = 6.38E-04). In the 'oxidative phosphorylation' pathway in particular, 95 genes were represented on the chips, out of which 24 genes were differentially expressed.

Q-RT-PCR validation

We used Q-RT-PCR assays to verify some of our microarray results. Five genes (*Atp5b* [F1-ATPase beta subunit]; *Col1a1* [collagen type 1 alpha 1]; *Cox6c* [cytochrome *c* oxidase subunit VIc]; *Ndufs3* [NADH dehydrogenase [ubiquinone] Fe-S protein 3] and *Tgfb1* [transforming growth factor beta 1]) were selected for verification because of their central positions in the most significantly enriched pathways. The expression ratios of these five genes, as determined through microarray and Q-RT-PCR, are shown in Table 7. All five genes were significantly increased in the DN group. Strong agreement between the microarray and Q-RT-PCR results was observed in all five genes, indicating the reliability of our microarray assays.

Renal expression of NDUFS3 and TGF-β1

Renal immunostaining for NDUFS3 and TGF-β1 expression in DN rats (Figures 3b and d) were elevated compared with the control group (Figure 3a and c). The expressions of NDUFS3 and TGF-β1 in the kidneys of DN rats were elevated. The semiquantitative score of NDUFS3 and TGF-β1 protein expressions in the DN group was increased significantly compared with those in the control group ($P < 0.05$, Figure 3e and f).

Discussion

DN is characterized by a set of diabetic pathophysiological changes.[18] In mammalian tissues, mRNA expressions are in a state of dynamic turnover in various development and pathophysiological states. In view of these considerations, we employed an expression profile gene array. This study represents the first attempt to understand the gene expression profiles in glomeruli from STZ-induced DN rats.

In our gene array research, DAVID analysis of all changed genes in the DN group yielded 21 GO categories. The third most enriched term was 'mitochondrion' (GO:0005739). After KEGG pathway analysis, all differentially expressed genes could be mapped to eight pathways. The fourth most significant pathway we found in the DN group was 'oxidative phosphorylation' (FDR = 6.77E-13). The results of Q-RT-PCR showed that *Atp5b*, *Cox6c* and *Ndufs3* were significantly increased in the DN group. The expression of NDUFS3 in the kidneys of DN rats was elevated. These findings suggest that the 'oxidative phosphorylation' pathway in the mitochondrion may play an important role in the development of DN.

In eukaryotic cells, mitochondria are important organelles. Through oxidative phosphorylation pathway, most

Table 6 KEGG pathway (fold enrichment > 2.0, FDR < 0.001)

KEGG_ID	Term	Count	Total number of genes in the pathway	Fold enrichment	FDR	Genes
rno04512	ECM–receptor interaction	26	72	7.869	3.89E-13	*Col3a1*, *Itgb4*, *Vtn*, *Sdc4*, *Sdc2*, *Gp9*, *Sdc3*, *Hmmr*, *Lamb2*, *Gp1bb*, *Tnr*, *Itgb6*, *Col6a2*, *Col6a1*, *Col11a1*, *Sv2c*, *Col4a2*, *Itga2*, *Itga3*, *Col5a3*, *Col5a2*, *Vwf*, *Lama1*, *Itga7*, *Lamc2*, *Col1a1*
rno03010	Ribosome	22	81	6.498	7.49E-09	*Rgd1566002*, *Rgd1563124*, *Rpl39*, *Rps25*, *Loc687780*, *Rpl30*, *Rps27*, *Rgd1561086*, *Rgd1560979*, *Arbp*, *Rps27a*, *Loc684988*, *Rpl35a*, *Rgd1565732*, *Rgd1562929*, *Rgd1563311*, *Rpl26*, *Rps6*, *Rgd1564744*, *Rgd1559574*, *Loc364236*, *Rgd1565370*, *Rgd1562601*, *Loc687298*, *Loc367923*, *Rgd1563543*, *Rgd1564423*
rno04510	Focal adhesion	29	98	3.646	3.67E-06	*Col3a1*, *Itgb4*, *Vtn*, *Pdpk1*, *Lamb2*, *Tnr*, *Itgb6*, *Ilk*, *Col6a2*, *Col6a1*, *Rhoc*, *Col11a1*, *Prkca*, *Col4a2*, *Flt1*, *Map2k1*, *Itga2*, *Prkcg*, *Itga3*, *Col5a3*, *Col5a2*, *Lama1*, *Vwf*, *Mapk1*, *Ccnd1*, *Vegfa*, *Itga7*, *Lamc2*, *Col1a1*
rno00190	Oxidative phosphorylation	24	95	4.295	4.91E-06	*Ndufb3*, *Loc688869*, *Cox6c*, *Ndufa5*, *Atp6ap1*, *Cox8a*, *Rgd1563463*, *Cox4i1*, *Atp5g2*, *Cox7a2l*, *Uqcrfs1*, *Ndufa1*, *Cox6c*, *Atp6v1c1*, *Sdha*, *Sdhb*, *Atp6v0e2*, *Uqcrh*, *Sdhc*, *Ndufv1*, *Atp6v1e1*, *Atp5c1*, *Ndufs3*, *Atp5j*, *Atp5b*
rno04350	TGF-beta signaling pathway	19	76	5.416	7.11E-06	*Ltbp1*, *Smad6*, *Bmpr2*, *Rps6kb2*, *Rps6kb1*, *Smad2*, *Skp1*, *Tgfb1*, *Rbx1*, *Mapk1*, *Acvr2b*, *Ep300*, *Sp1*, *Id1*, *Zfyve9*, *Lefty2*, *Rhoc*, *Bmpr1b*, *Bmp7*
rno05012	Parkinson's disease	22	97	3.798	2.35E-04	*Ndufb3*, *Loc688869*, *Cox6c*, *Ndufa5*, *Cox8a*, *Rgd1563463*, *Cox4i1*, *Atp5g2*, *Cox7a2l*, *Uqcrfs1*, *Ndufa1*, *Vdac3*, *Cox6c*, *Sdha*, *Sdhb*, *Uqcrh*, *Gp1bb*, *Sdhc*, *Ndufv1*, *Atp5c1*, *Ndufs3*, *Atp5j*
rno05010	Alzheimer's disease	26	144	3.235	3.28E-04	*Ndufb3*, *Rgd1560581*, *Cox6c*, *Hsd17b10*, *Rgd1563463*, *Mme*, *Atp5g2*, *Cox7a2l*, *Uqcrfs1*, *Rgd1565137*, *Rgd1565891*, *Cabc1*, *Ndufs3*, *Rgd1562758*, *Atp5j*, *Loc688869*, *Ndufa5*, *Cox8a*, *Cox4i1*, *Loc361841*, *Ndufa1*, *Rgd1565368*, *Cox6c*, *Sdha*, *Mapk1*, *Sdhb*, *Rgd1565238*, *Uqcrh*, *Sdhc*, *Ndufv1*, *Rgd1559704*, *Atp5c1*, *Calm3*
rno04614	Renin–angiotensin system	9	23	11.032	6.38E-04	*Agtr2*, *Ace*, *Agtr1b*, *Agtr1a*, *Agt*, *Thop1*, *Ace2*, *Cpa3*, *Mme*

FDR, false discovery rate; ECM, extracellular matrix; KEGG, Kyoto Encyclopedia of Genes and Genomes

of the ATP is generated from mitochondria. Mitochondria are also a major cellular source for reactive oxygen species (ROS). Some evidences have shown that increased oxidative stress contributes to DN development.[19–21] Hyperglycemia increases ROS production through the mitochondrial electron transport chain in mesangial cells.[22] When primary renal proximal tubule cells (PTCs) were cultured in the presence of high glucose, H_2O_2 was increased. Apocynin, diphenylene iodonium (NADPH oxidase inhibitors) and rotenone (inhibitor of complex I of the mitochondrial electron transport chain) effectively block the high glucose-induced generation of H_2O_2 in renal PTCs.[23] Moreover, hyperglycemia increases the production of ROS inside cultured bovine aortic endothelial cells.[21] This increase in ROS is prevented by an inhibitor of electron transport chain complex II, by an uncoupler of oxidative phosphorylation, by uncoupling protein-1 and by manganese superoxide dismutase. Normalizing levels of mitochondrial ROS with each of these agents prevents the development and progression of diabetic complications.[21]

Table 7 Fold change in gene expression measured by gene array and Q-RT-PCR

Gene symbols	Fold change (microarray)	Fold change (Q-RT-PCR)	*P* value (Q-RT-PCR)
Atp5b	4.553	3.9	0.039
Col1a1	4.833	4.3	0.003
Cox6c	7.127	7.2	0.004
Ndufs3	3.989	3.2	0.013
Tgfb1	2.907	3.1	0.001

Atp5b, F1-ATPase beta subunit; *Col1a1*, collagen type 1 alpha 1; *Cox6c*, cytochrome c oxidase subunit VIc; *Ndufs3*, NADH dehydrogenase (ubiquinone) Fe-S protein 3; *Tgfb1*, transforming growth factor beta 1; Q-RT-PCR, quantitative realtime polymerase chain reaction

A great deal of data shows four main hypotheses on how hyperglycemia causes DN, and several trials based on specific inhibitors support these mechanisms. The four hypotheses are: increased polyol pathway flux; increased advanced glycation end-product formation; activation of protein kinase C isoforms; and increased hexosamine pathway flux. Recently, Brownlee[24] proposed a unified mechanism that overproduction of superoxide by the mitochondrial electron-transport chain activates the four pathways despite the absence of hyperglycemia.

The most significant pathway we found was the 'ECM–receptor interaction' (FDR = 3.89E-13). The result of Q-RT-PCR showed that *Col1a1* was significantly increased in the DN group. Key features of DN include the

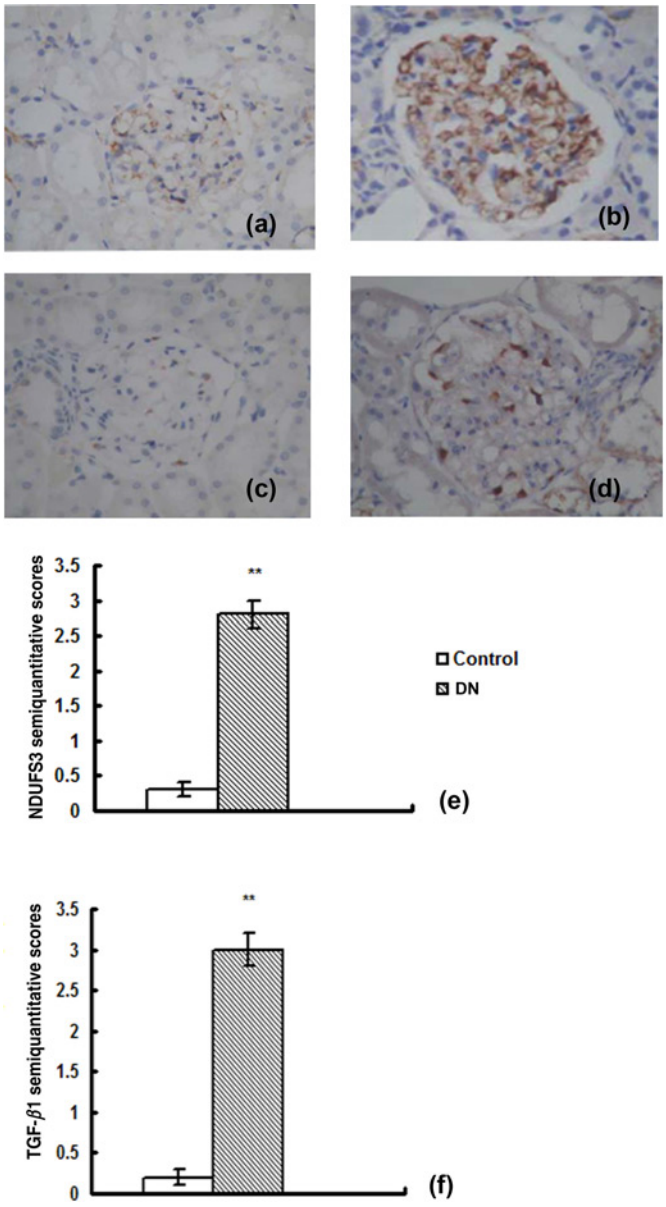

Figure 3 Renal immunohistochemistry for NDUFS3 and transforming growth factor beta 1 (TGF-β1) expression (original magnification, 200×) and semiquantitative assessments. a–b: immunostaining for NDUFS3. c–d: immunostaining for TGF-β1. Kidney tissues were harvested from control (a, c) and diabetic nephropathy (b, d) group. Semiquatitative scores of the immunostaining for NDUFS3 protein (e) and TGF-β1 (f) were scored using four levels, and an average value was obtained from analyses of more than 30 glomeruli per rat. The images were taken at the same size. Data represent mean ± SD ($n = 10$). $^{*}P < 0.05$, $^{**}P < 0.01$ versus the control group. (A colour version of this figure is available in the online journal)

accumulation of ECM proteins, such as Col1a1. Previous studies have shown that Col1a1 and other ECM genes are regulated in mesangial cells by TGF-β via Smads.[25,26]

The present study also identified disruptions in TGF-β signaling in DN rats. Q-RT-PCR and renal immunostaining have verified this result. TGF-β is a cytokine which belongs to a large superfamily of activins/bone morphogenetic proteins.[27] This mediator plays an active role in proliferation, wound healing[28] and synthesis of ECM molecules.[29] The TGF-β level is elevated in the kidneys of insulin-dependent diabetic animals during both early and late stages of disease.[30,31] Treatment of the STZ-diabetic rat with sufficient insulin to reduce hyperglycemia suppressed the enhanced expression of TGF-β and matrix components in the glomeruli. In the STZ-diabetic rat and mouse, the expression of TGF-β increased in the renal cortex and glomeruli early after the onset of diabetes.[30] The db/db mouse, a model of type 2 diabetes, characterized by hyperglycemia, obesity, and insulin resistance, develops increased amounts of TGF-β1 localized in the glomerular compartments.[32]

Nine of 23 genes were differently expressed in the 'RAS' pathway. The RAS plays crucial roles in cardiovascular and renal pathophysiology. Angiotensin II (Ang II) binds to its two major high-affinity receptors, designated AT1 and AT2. Signaling through the AT1 receptor results in vasoconstriction and sodium reabsorption, and also promotes cellular growth, hypertrophy, activation of fibroblasts, and ECM deposition in the kidney. Recently, randomized clinical trials have demonstrated that an AT1 receptor antagonist, losartan, has significant renoprotective effects on non-diabetic as well as diabetic nephropathy.[33] Ang II seems to play one of the central roles in the pathogenesis of renal interstitial fibrosis.[34] An analysis of AT1a gene knockout mice demonstrated the inhibitory effect of AT1 blockade on renal interstitial fibrosis.[35] Several experimental studies suggest that the concentration of Ang II in the renal interstitium may be 60–100-fold higher than that in the circulation.[36] Therefore, RAS may have an important role in the progression of DN.

In summary, our studies provide the evidence that DN may be involved with the oxidative phosphorylation pathway, ECM-receptor interaction, TGF-β pathway and RAS. These results provide molecular information for further investigation of the mechanisms of DN development. Furthermore, these results could be important in devising mechanism-based and targeted therapeutic strategies for DN and kidney dysfunction.

Author contributions: XX designed the experiments, analyzed the data, interpreted the results and reviewed the manuscript. QZ co-designed the study, conducted the experiments, co-analyzed the data and wrote the paper. ML, WL, MY, HZ, XS, LM and HX contributed reagents/materials/analysis tools.

ACKNOWLEDGEMENTS

This study was funded by grants from the foundation of Peking Union Medical College Hospital (No. 2006119) and National Clinical Key Specialty Construction Projects.

REFERENCES

1 Wild S, Roglic G, Green A, Sicree R, King H. Global prevalence of diabetes: estimates for the year 2000 and projections for 2030. *Diabetes Care* 2004;**27**:1047–53

2 Wu AY, Kong NC, de Leon FA, Pan CY, Tai TY, Yeung VT, Yoo SJ, Rouillon A, Weir MR. An alarmingly high prevalence of diabetic

nephropathy in Asian type 2 diabetic patients: the MicroAlbuminuria Prevalence (MAP) Study. *Diabetologia* 2005;**48**:17–26
3 Dalla Vestra M, Saller A, Bortoloso E, Mauer M, Fioretto P. Structural involvement in type 1 and type 2 diabetic nephropathy. *Diabetes Metab* 2000;**26**:8–14
4 Kanwar YS, Wada J, Sun L, Xie P, Wallner EI, Chen S, Chugh S, Danesh FR. Diabetic nephropathy: mechanisms of renal disease progression. *Exp Biol Med* 2008;**233**:4–11
5 Ritz E, Orth SR. Nephropathy in patients with type 2 diabetes mellitus. *N Engl J Med* 1999;**341**:1127–33
6 White KE, Marshall SM, Bilous RW. Prevalence of atubular glomeruli in type 2 diabetic patients with nephropathy. *Nephrol Dial Transplant* 2008;**23**:3539–45
7 Wada J, Zhang H, Tsuchiyama Y, Hiragushi K, Hida K, Shikata K, Kanwar YS, Makino H. Gene expression profile in streptozotocin-induced diabetic mice kidneys undergoing glomerulosclerosis. *Kidney Int* 2001;**59**:1363–73
8 Wilson KH, Eckenrode SE, Li QZ, Ruan QG, Yang P, Shi JD, Davoodi-Semiromi A, Mclndoe RA, Croker BP, She JX. Microarray analysis of gene expression in the kidneys of new- and post-onset diabetic NOD mice. *Diabetes* 2003;**52**:2151–9
9 Onozato ML, Tojo A, Leiper J, Fujita T, Palm F, Wilcox CS. Expression of NG, NG-dimethylarginine dimethylaminohydrolase and protein arginine *N*-methyltransferase isoforms in diabetic rat kidney: effects of angiotensin II receptor blockers. *Diabetes* 2008;**57**:172–80
10 Schlondorff D. Preparation and study of isolated glomeruli. *Methods Enzymol* 1990;**191**:130–40
11 Border WA, Okuda S, Languino LR, Sporn MB, Ruoslahti E. Suppression of experimental glomerulonephritis by antiserum against transforming growth factor beta 1. *Nature* 1990;**346**:371–4
12 Benjamini Y, Hochberg Y. Controlling the false discovery rate: a practical and powerful approach to multiple testing. *J R Stat Soc Ser B* 1995;**57**:289–300
13 Eisen MB, Spellman PT, Brown PO, Botstein D. Cluster analysis and display of genome-wide expression patterns. *Proc Natl Acad Sci USA* 1998;**95**:14863–8
14 Dennis G Jr, Sherman BT, Hosack DA, Yang J, Gao W, Lane HC, Lempicki RA. DAVID: database for annotation, visualization, and integrated discovery. *Genome Biol* 2003;**4**:P3
15 Hosack DA, Dennis G Jr, Sherman BT, Lane HC, Lempicki RA. Identifying biological themes within lists of genes with EASE. *Genome Biol* 2003;**4**:R70
16 Livak KJ, Schmittgen TD. Analysis of relative gene expression data using real-time quantitative PCR and the 2(-Delta DeltaC(T)) method. *Methods* 2001;**25**:402–8
17 Gross ML, EI-Shakmak A, Szabo A, Koch A, Kuhlmann A, Munter K, Ritz E, Amann K. ACE-inhibitors but not endothelin receptor blockers prevent podocyte loss in early diabetic nephropathy. *Diabetologia* 2003;**46**:856–68
18 Kanwar YS, Sun L, Xie P, Liu FY, Chen S. A glimpse of various pathogenetic mechanisms of diabetic nephropathy. *Annu Rev Pathol* 2011;**6**:395–423
19 Brownlee M. Biochemistry and molecular cell biology of diabetic complications. *Nature* 2001;**414**:813–20
20 Du XL, Edelstein D, Dimmeler S, Ju Q, Sui C, Brownlee M. Hyperglycemia inhibits endothelial nitric oxide synthase activity by posttranslational modification at the Akt site. *J Clin Invest* 2001;**108**:1341–8
21 Nishikawa T, Edelstein D, Du XL, Yamagishi S, Matsumura T, Kaneda Y, Yorek MA, Beebe D, Oates PJ, Hammes HP, Giardino I, Brownlee M. Normalizing mitochondrial superoxide production blocks three pathways of hyperglycaemic damage. *Nature* 2000;**404**:787–90
22 Kiritoshi S, Nishikawa T, Sonoda K, Kukidome D, Senokuchi T, Matsuo T, Matsumura T, Tokunaga H, Brownlee M, Araki E. Reactive oxygen species from mitochondria induce cyclooxygenase-2 gene expression in human mesangial cells: potential role in diabetic nephropathy. *Diabetes* 2003;**52**:2570–7
23 Han HJ, Lee YJ, Park SH, Lee JH, Taub M. High glucose-induced oxidative stress inhibits Na^+/glucose cotransporter activity in renal proximal tubule cells. *Am J Physiol Renal Physiol* 2005;**288**:F988–96
24 Brownlee M. The pathobiology of diabetic complications: a unifying mechanism. *Diabetes* 2005;**54**:1615–25
25 Kato M, Arce L, Wang M, Putta S, Lanting L, Natarajan R. A microRNA circuit mediates transforming growth factor-β1 autoregulation in renal glomerular mesangial cells. *Kidney Int* 2011;**80**:358–68
26 Kato M, Zhang J, Wang M, Lanting L, Yuan H, Rossi JJ, Natarajan R. MicroRNA-192 in diabetic kidney glomeruli and its function in TGF-beta-induced collagen expression via inhibition of E-box repressors. *Proc Nat Acad Sci USA* 2007;**104**:3432–7
27 Shi Y, Massague J. Mechanisms of TGF-beta signaling from cell membrane to the nucleus. *Cell* 2003;**113**:685–700
28 Faler BJ, Macsata RA, Plummer D, Mishra L, Sidawy AN. Transforming growth factor-beta and wound healing. *Perspect Vasc Surg Endovasc Ther* 2006;**18**:55–62
29 Hocevar BA, Howe PH. Analysis of TGF-beta-mediated synthesis of extracellular matrix components. *Methods Mol Biol* 2000;**142**:55–65
30 Yamamoto T, Nakamura T, Noble NA, Ruoslahti E, Border WA. Expression of transforming growth factor beta is elevated in human and experimental diabetic nephropathy. *Proc Natl Acad Sci USA* 1993;**90**:1814–8
31 Sharma K, Ziyadeh FN. Renal hypertrophy is associated with upregulation of TGF-beta 1 gene expression in diabetic BB rat and NOD mouse. *Am J Physiol* 1994;**267**:F1094–01
32 Hong SW, Isono M, Chen S, Iglesias-De La Cruz MC, Han DC, Ziyadeh FN. Increased glomerular and tubular expression of transforming growth factor-beta1, its type II receptor, and activation of the Smad signaling pathway in the db/db mouse. *Am J Pathol* 2001;**158**:1653–63
33 Nakao N, Yoshimura A, Morita H, Takada M, Kayano T, Ideura T. Combination treatment of angiotensin-II receptor blocker and angiotensin-converting-enzyme inhibitor in non-diabetic renal disease (COOPERATE): a randomised controlled trial. *Lancet* 2003;**361**:117–24
34 Klahr S, Morrissey J. Obstructive nephropathy and renal fibrosis. *Am J Physiol Renal Physiol* 2002;**283**:F861–75
35 Satoh M, Kashihara N, Yamasaki Y, Maruyama K, Okamoto K, Maeshima Y, Sugiyama H, Sugaya T, Murakami K, Makino H. Renal interstitial fibrosis is reduced in angiotensin II type 1a receptor-deficient mice. *J Am Soc Nephrol* 2001;**12**:317–25
36 van Kats JP, Schalekamp MA, Verdouw PD, Duncker DJ, Danser AH. Intrarenal angiotensin II: interstitial and cellular levels and site of production. *Kidney Int* 2001;**60**:2311–7

(Received January 22, 2012, Accepted April 27, 2012)